

UNCLASSIFIED

AD NUMBER

AD909543

LIMITATION CHANGES

TO:

Approved for public release; distribution is unlimited. Document partially illegible.

FROM:

Distribution authorized to U.S. Gov't. agencies only; Test and Evaluation; MAR 1973. Other requests shall be referred to Naval Research Laboratory, Washington, DC 20375. Document partially illegible.

AUTHORITY

USNRL ltr, 31 Dec 1975

THIS PAGE IS UNCLASSIFIED

AD 909543

LIBRARY  
TECHNICAL REPORT SECTION  
NAVAL POSTGRADUATE SCHOOL  
MONTEREY, CALIFORNIA 93940 93943

NRL Report 7533

# Performance of Cascaded MTI and Coherent Integration Filters in a Clutter Environment

G. A. ANDREWS, JR.

Airborne Radar Branch  
Radar Division

March 27, 1973

Classification category of document

Approved for Public Release, Distribution Unlimited  
by authority of  
Naval Research Laboratory Letter dated

31 Dec 1975

(Date)

(Signature)

Caroline J. Mills, GS-4

Naval Postgraduate School



NAVAL RESEARCH LABORATORY

Washington, D.C.

Distribution limited to U.S. Government Agencies only; test and evaluation, March 1973. Other requests for this document must be referred to the Director, Naval Research Laboratory, Washington, D.C. 20375

APPROVED FOR PUBLIC RELEASE, DISTRIBUTION UNLIMITED

36P

THIS REPORT HAS BEEN DELIMITED  
AND CLEARED FOR PUBLIC RELEASE  
UNDER DOD DIRECTIVE 5200.20 AND  
NO RESTRICTIONS ARE IMPOSED UPON  
ITS USE AND DISCLOSURE.

**DISTRIBUTION STATEMENT A**

APPROVED FOR PUBLIC RELEASE;  
DISTRIBUTION UNLIMITED.



## NAVAL RESEARCH LABORATORY

~~WASHINGTON, D.C. 20375~~  
WASHINGTON, D.C. 20375

IN REPLY REFER TO:  
2628-695:HW0:dar

DEC 31 1975

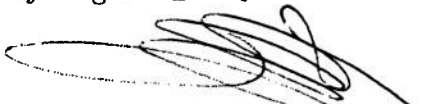
From: Director, U.S. Naval Research Laboratory, Washington, DC 20375  
To: All Holders of NRL Report 7533

Subj: Distribution Statement for unclassified NRL Report 7533,  
"PERFORMANCE OF CASCADED MTI AND COHERENT INTEGRATION FILTERS  
IN A CLUTTER ENVIRONMENT," by G.A. Andrews, Jr., dtd  
March 27, 1973; change of

1. The current Distribution Statement indicated in subject report is changed from "Distribution limited to U.S. Government Agencies only; test and evaluation; March 1973. Other requests for this document must be referred to the Director, Naval Research Laboratory, Washington, D.C. 20390" to Unlimited Statement "A" to read as follows:

"APPROVED FOR PUBLIC RELEASE; DISTRIBUTION UNLIMITED."

2. It is requested that notation of this Unlimited Distribution Statement be marked on all copies of subject report in accordance with appropriate departmental security regulations.

  
H. W. OTTENSTROER  
By direction

## CONTENTS

|   |    |
|---|----|
| Abstract .....                                | ii |
| Authorization .....                           | ii |
| I. INTRODUCTION .....                         | 1  |
| II. GENERALIZED PROCESSOR MODEL .....         | 2  |
| Matrix Equivalent .....                       | 2  |
| Expected Output Clutter Power .....           | 3  |
| Expected Output Signal Power .....            | 4  |
| Improvement Factor .....                      | 6  |
| III. MTI FILTERS .....                        | 6  |
| IV. COHERENT INTEGRATOR (FFT) .....           | 8  |
| Uniform Weights .....                         | 8  |
| Tschebyshev Weights .....                     | 12 |
| V. CASCADED MTI AND COHERENT INTEGRATOR ..... | 12 |
| Optimum Cascaded Filters .....                | 12 |
| Matrix Equations For Cascaded Filters .....   | 15 |
| Transfer Function .....                       | 18 |
| Improvement Factor .....                      | 18 |
| VI. CONCLUSIONS .....                         | 30 |
| VII. ACKNOWLEDGMENT .....                     | 31 |
| VIII. REFERENCES .....                        | 31 |

## ABSTRACT

The combination of moving target indicator (MTI) and coherent integration filters can provide velocity filtering with advantages that neither technique can provide alone. These techniques are evaluated as a special case of a transversal filter which lends itself to analysis using matrix algebra. This approach gives a simple, easily understood insight into the effects of weighting the input radar data. The resulting matrix equations are evaluated and the results are plotted for some special configurations. The computer programs which were written as a part of this research are not restricted to these configurations nor to the type of clutter spectrum that is assumed.

It is shown that the performance of coherent integrators in a coherent noise (clutter) environment cannot be predicted with a concise analytical expression. In particular, the weighing of the input data and the covariance matrix of the interference determine the integrator performance.

## AUTHORIZATION

NRL Problem R02-29  
Project A360-5333/652B/2F00-141-601

Manuscript submitted November 28, 1972.

## PERFORMANCE OF CASCADED MTI AND COHERENT INTEGRATION FILTERS IN A CLUTTER ENVIRONMENT

### I. INTRODUCTION

Recent advances in velocity filtering for radar systems have been made possible mainly through the use of digital signal processing. The detection of moving targets in the presence of strong returns from fixed objects (clutter) has classically been accomplished with moving target indicators (MTI) or with pulse doppler radars (Chap. 17 and 19, Ref. 1). The flexibility of digital signal processing allows improved implementation of both techniques, as well as processing configurations which make use of the advantages of both.

MTI is normally used with low-pulse-repetition-frequency (low-PRF) radars. The MTI filter rejects clutter by means of a notch in its passband centered on the clutter doppler spectrum. A single output provides moving target detection over the remaining doppler spectrum between the PRF harmonics. Pulse doppler is usually associated with high-PRF radars. A contiguous bank of narrow-band filters is used to detect moving targets outside of the clutter spectrum.

A pulse doppler radar can usually achieve a greater improvement in the signal-to-clutter ratio than can an MTI. This improvement is needed to contend with the higher clutter levels caused by clutter foldover at the range ambiguities of the high-PRF pulse doppler radar. The increased clutter rejection results from the high PRF and from the larger number of pulses processed by the pulse doppler radar.

McAulay (2) formulated the MTI problem as a classical detection problem. He determined the optimum process by maximizing the resulting likelihood ratio and showed that the optimum receiver structure could be interpreted as a clutter filter in cascade with a narrow-band doppler filter bank. This arrangement has the advantage that the dynamic range at the input to the narrowband processor is greatly reduced by the clutter rejection of the clutter filter.

A practical approximation to this processor consists of a conventional MTI filter cascaded with a coherent integrator formed by a contiguous bank of narrow-band filters. The coherent integrator has been implemented by using the Fast Fourier Transform (FFT) algorithm (3,4). The processing gain, i.e., the improvement in signal-to-clutter ratio that can be achieved by this configuration, is considered in this report.

The improvement factor that can be achieved using an MTI alone, and then a coherent integrator alone, is presented first. This gives a basis for comparing the advantages of cascading the two filters. A Gaussian clutter spectrum is assumed in computing the improvement factors. Although not completely accurate, this assumption is generally made in the MTI literature and it has been found to give a reasonable prediction of MTI performance.

In general, the number of pulses that can be coherently processed is limited by the number of pulses that are transmitted during the antenna dwell time. This number can range from one or two to several hundred, depending on the particular radar application. In practice, the number of pulses may be constrained by the cost, weight, or size of the processor hardware. In this report, the MTI filters are considered to be single, double, or triple cancellers. The coherent integrators are considered to be 8- or 16-pulse FFTs; the weights used to shape the FFT filter response are either uniform (all weights equal) or Tschhebyshev (-25 dB sidelobes). These choices seem to be typical of the processors that might be considered for many low-PRF radars. However, the computer programs used to evaluate these processors are neither restricted by these choices nor by the assumed Gaussian clutter spectrum.

## II. GENERALIZED PROCESSOR MODEL

### Matrix Equivalent

Both the MTI and the coherent integrator can be modeled as a transversal filter of the type shown in Fig. 1. A tapped delay line (or multiple delay lines) is used to provide  $n+1$  time samples of the input  $x(t)$ . The output  $y(t)$  consists of a weighted sum of these samples:

$$y(t) = W_1 x(t) + W_2 x(t - T) + \dots + W_{n+1} x(t - nT) \quad (1)$$

where  $T$  is the time between samples.  $x(t)$ ,  $y(t)$ , and the weights  $W_i$  may be complex.

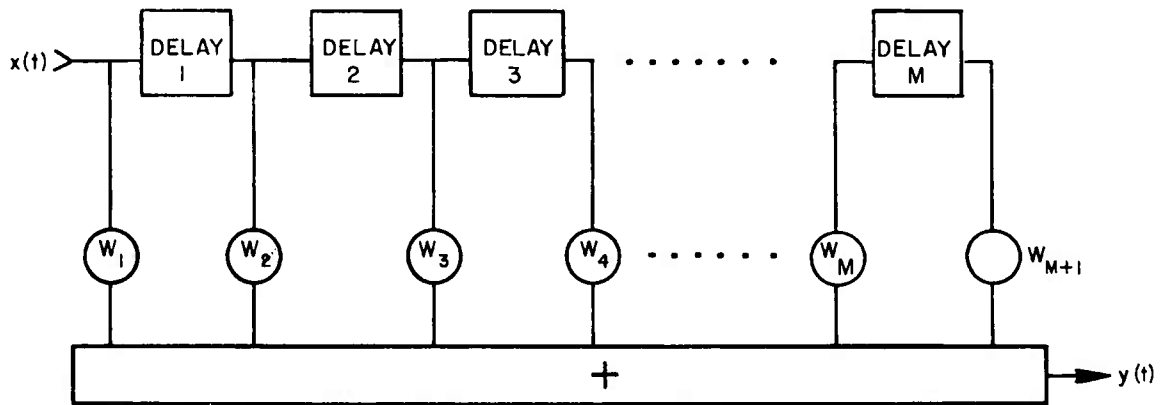


Fig. 1 — Generalized model for an MTI or coherent integrator processor consisting of a single filter and a single output

For purposes of analysis, it is convenient to write Eq. (1) as a matrix operation. Therefore, define  $W$  and  $X$  as column vectors with elements given by



$$W = \begin{bmatrix} W_1 \\ W_2 \\ W_3 \\ . \\ . \\ . \\ W_{n+1} \end{bmatrix} \quad \text{and} \quad X = \begin{bmatrix} x_1 \\ x_2 \\ x_3 \\ . \\ . \\ . \\ x_{n+1} \end{bmatrix}$$

where  $W_i$  is the  $i$ th weight shown in Fig. 1, and

$$\begin{aligned} x_1 &= x(t) \\ x_2 &= x(t-T) \\ x_3 &= x(t-2T) \\ . & \\ . & \\ . & \\ x_{n+1} &= x(t-nT). \end{aligned}$$

With these matrices, Eq. (1) can be written as the product of the transpose of  $W$ ,  $W_T$ , times  $X$ :

$$y = W_T X.$$

The output power, as shown in Ref. 5, is given by

$$\begin{aligned} P &= |y|^2 = yy^* = yy_T^* \\ &= W_T X (W_T X)^* \\ &= W_T X X_T^* W \end{aligned} \tag{2}$$

where use has been made of the fact that

$$y_T = y.$$

The output signal-to-clutter ratio can be computed by taking the ratio of Eq. (2) when  $x(t)$  is the input signal to Eq. (2) when  $x(t)$  is the input clutter.

#### Expected Output Clutter Power

The expected output clutter power  $\bar{P}_c$  is found from the expected value of Eq. (2):

$$\bar{P}_c = E \{ W_T X X_T^* W^* \} = W_T \overline{X X_T^*} W^*. \quad (3)$$

Letting

$$M_c = \overline{X X_T^*}$$

Then

$$\bar{P}_c = W_T M_c W^* \quad (4)$$

where  $M_c$ , the covariance matrix of the clutter, can be derived from the Fourier transform of the normalized clutter power density spectrum. For example, using a Gaussian clutter spectrum yields

$$P_c(f) = \frac{1}{\sqrt{2\pi} \sigma_c} e^{-\frac{1}{2} \left( \frac{f - \mu_c}{\sigma_c} \right)^2}. \quad (5)$$

The mean  $\mu_c$  implies relative motion between the radar platform and the clutter. The standard deviation  $\sigma_c$  of the clutter spectrum is a measure of the bandwidth of the clutter spectrum.

The Fourier transform of Eq. (5) is

$$\psi(\tau) = \exp(-2\pi^2 \sigma_c^2 \tau^2 - j 2\pi \mu_c \tau).$$

Assuming stationarity, the  $k, l$  element of  $M_c$  is

$$M_c(k, l) = \exp[-2\pi^2 \sigma_c^2 (k - l)^2 T^2 - j 2\pi \mu_c (k - l) T]. \quad (6)$$

#### Expected Output Signal Power

Letting the input  $x(t)$  correspond to a signal input, the expected output signal power  $P_s$  is found in the same way as above for the clutter:

$$P_s = W_T M_s W^* \quad (7)$$

where  $M_s$  is the covariance matrix for the signal. The spectrum of a target is affected by such things as the target's characteristics, transmitted waveform, radar stability, antenna scanning, and relative velocity. The received signal waveform  $r(t)$  is given by

$$r(t) = s(t) e^{j\omega_d t} \quad (8)$$

where  $s(t)$  includes all the above effects, except relative velocity, and  $\omega_d$  is the doppler frequency corresponding to the relative velocity between radar and target. Since no apriori knowledge is assumed about  $\omega_d$ , it is given a uniform probability distribution ( $0 \leq \omega_d \leq \text{PRF}$ ).

If the doppler shift is the dominant effect, i.e., the bandwidth of the other effects are small relative to the doppler shifts expected, then Eq. (8) is approximately

$$r(t) = e^{j\omega_d t}. \quad (9)$$

The autocorrelation of Eq. (9) is

$$\psi(\tau) = e^{j\omega_d \tau}. \quad (10)$$

The processor shown in Fig. 1 depicts only one filter and one output. However, in general, multiple independent outputs are possible by selecting appropriate weight vectors. In particular, the FFT weights form  $n+1$  filters with  $n+1$  outputs. The signal gain of a particular filter then will be the expected gain, provided that  $\omega_d$  is such that a signal exists somewhere between the crossover points of adjacent filters. This is shown in Fig. 2 for an 8-pulse FFT.

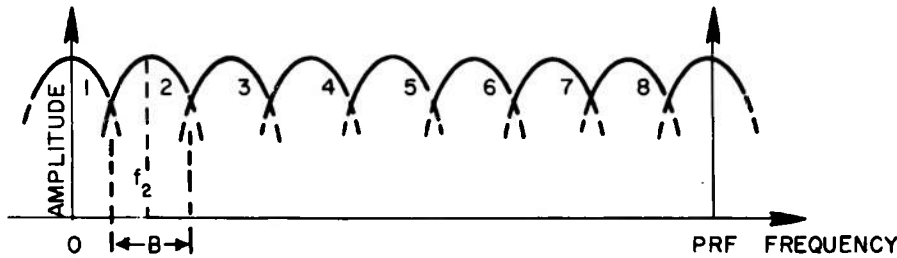


Fig. 2 — Signal amplitude vs PRF for a multiple-filter, multiple-output integrator. The case illustrated here is for an 8-pulse FFT.

From Fig. 2, the gain of the second filter is derived by considering a target doppler  $f_d$  that can occur with equal probability in the region

$$f_2 - (B/2) \leq f_d \leq f_2 + (B/2)$$

where  $f_2$  is the center of the response of the second filter.

The gain of the  $i$ th filter is derived in the same way by considering the region

$$f_i - (B/2) \leq f_d \leq f_i + (B/2).$$

The probability density function for  $f_d$  associated with the  $i$ th filter is

$$P(f_d) = \begin{cases} 1/B, & \text{for } (f_i - B/2) \leq f_d \leq (f_i + B/2) \\ 0, & \text{elsewhere.} \end{cases}$$

The expected value of Eq. (10) is

$$E \{ \psi(\tau) \} = \int_{-\infty}^{\infty} e^{j2\pi f_d \tau} P(f_d) df_d = e^{j2\pi f_i \tau} \frac{\sin(\pi B \tau)}{\pi B \tau}. \quad (11)$$

Assuming stationarity, the  $k, l$  element of the signal covariance matrix  $M_s$  is given by

$$m_s(k, l) = \exp [j2\pi f_i(k - l) T] \frac{\sin [\pi B(k - l) T]}{\pi B(k - l) T}. \quad (12)$$

### Improvement Factor

The processing gain of any arbitrary transversal filter specified by a weight vector  $W$  can be computed by taking the ratio of the signal output power [Eq. (7)] to the clutter output power [Eq. (4)]. The processing gain, or improvement factor  $I$ , is

$$I = \frac{W_T M_s W^*}{W_T M_c W^*}. \quad (13)$$

The matrix  $M_s$  is generated from Eq. (12), and  $M_c$  is generated from Eq. (6).

### III. MTI FILTERS

A simplified diagram of an  $n$ -stage MTI is shown in Fig. 3. This diagram is equivalent to the model in Fig. 1 if the weights are given by the binomial coefficients with alternating signs, i.e.,

$$w_i = (-1)^{i-1} \binom{n}{i-1}, \quad i = 1, 2, \dots, n+1.$$

Using these weights in Eq. (7), the power transfer function can be computed by setting the bandwidth  $B$  equal to zero in Eq. (12) and varying  $f_i$  from zero to  $1/T$ , where  $1/T$  is the PRF. This corresponds to a sine wave input varying from zero to the PRF. The normalized power transfer function  $P_s$ , as defined in Eq. (7), is found for  $n = 1$  to  $n = 7$ , and the results are as shown in Fig. 4.

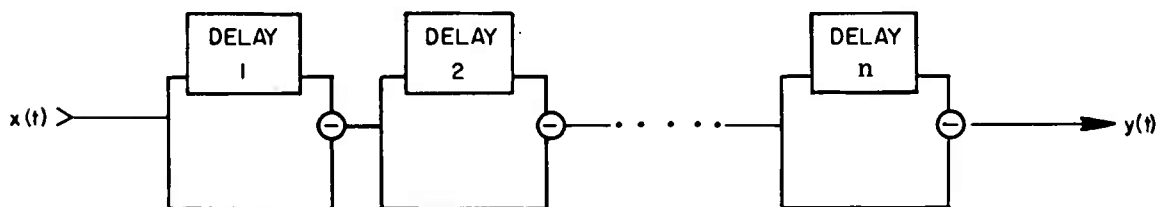


Fig. 3 — An  $n$ -stage, or  $n$ -canceller, MTI

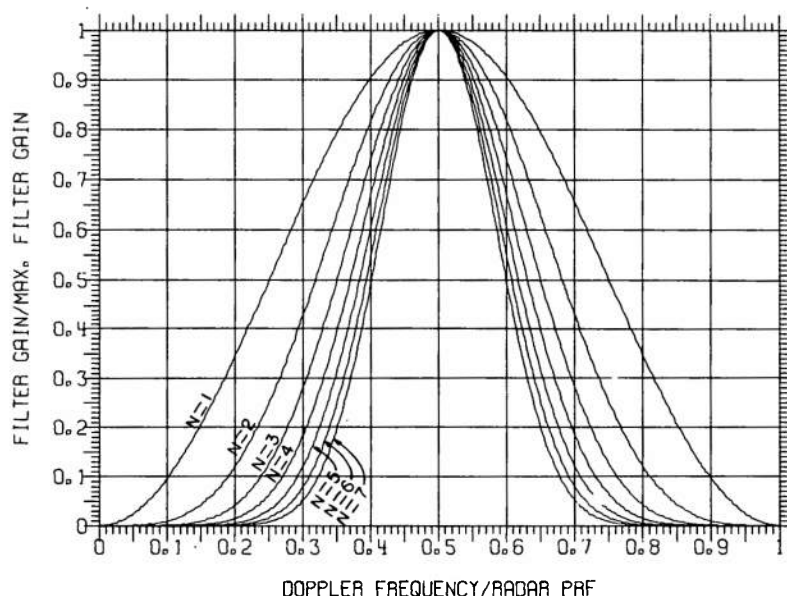


Fig. 4 — Normalized power transfer function  $P_s$  for an MTI having the indicated number of cancellers

The power transfer function is normalized by dividing by the maximum gain  $W_N$  given by

$$W_N = \sum_{i=1}^{n+1} W_i^2.$$

The maximum gain  $W_N$  is listed below for  $n = 1$  to  $n = 7$ :

| $n$ | $W_N$ |
|-----|-------|
| 1   | 2     |
| 2   | 6     |
| 3   | 20    |
| 4   | 70    |
| 5   | 252   |
| 6   | 923   |
| 7   | 3432  |

The improvement factor for an  $n$ -stage MTI is obtained by using Eq. (13). The matrix  $M_s$  is generated by letting  $B = 1/T$  in Eq. (12), i.e., the target doppler may occur at any frequency from zero to the PRF (PRF =  $1/T$ ). Also, let  $f_i = 1/2T$ , i.e., the center of the filter is at one-half the PRF. The covariance matrix  $M_n$  is generated using Eq. (6), with the average clutter doppler  $\mu_c$  equal to zero. The results are plotted in Fig. 5, where the clutter spectral width  $\sigma_c$  ranges from  $10^{-3}$  to  $10^{-1}$  times the PRF. Curves similar to Fig. 5 have been derived using various methods and published in several places (6,7).

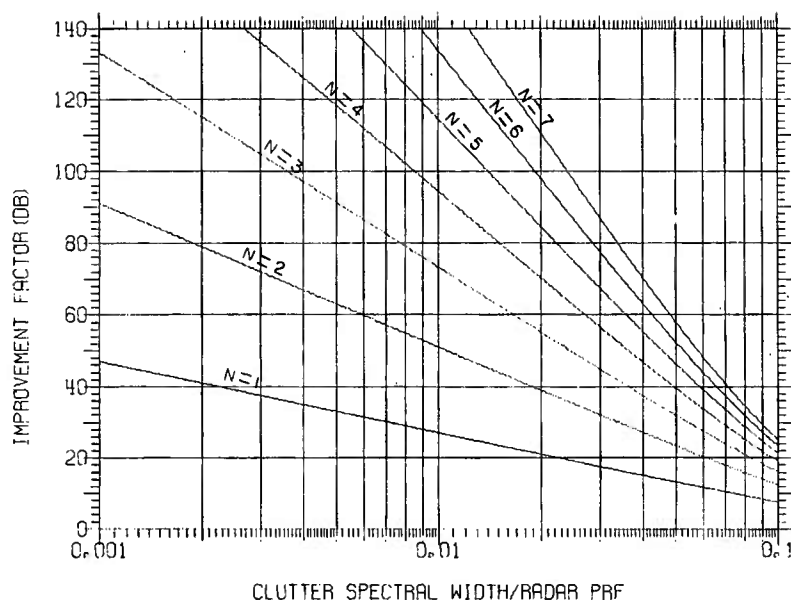


Fig. 5 — Improvement factor  $I$  [given by Eq. (13)] for an MTI having the indicated number of cancellers (filters)

#### IV. COHERENT INTEGRATOR (FFT)

##### Uniform Weights

The discrete Fourier transform can be characterized by

$$y_k = \sum_{n=1}^N x_n e^{-j2\pi \frac{(n-1)(k-1)}{N}}, \quad k = 1, 2, \dots, N \quad (14)$$

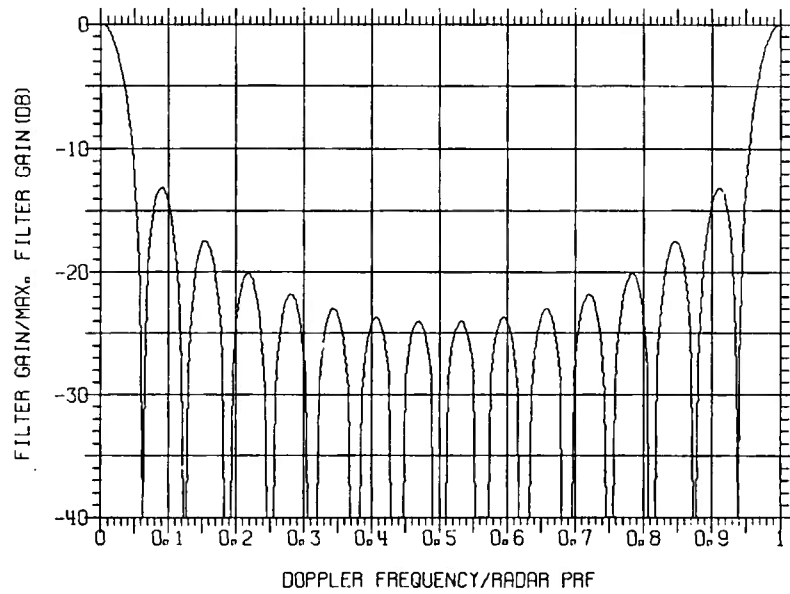
where  $x_n$  is the input time sample, and the  $y_k$  are the output spectral components. Therefore, Eq. (14) describes  $N$  filters with outputs  $y_1, y_2, \dots, y_N$ , as sketched in Fig. 2. The effective weights of the  $k$ th filter are

$$W_{kn} = e^{-j2\pi \frac{(n-1)(k-1)}{N}}, \quad n = 1, 2, \dots, N. \quad (15)$$

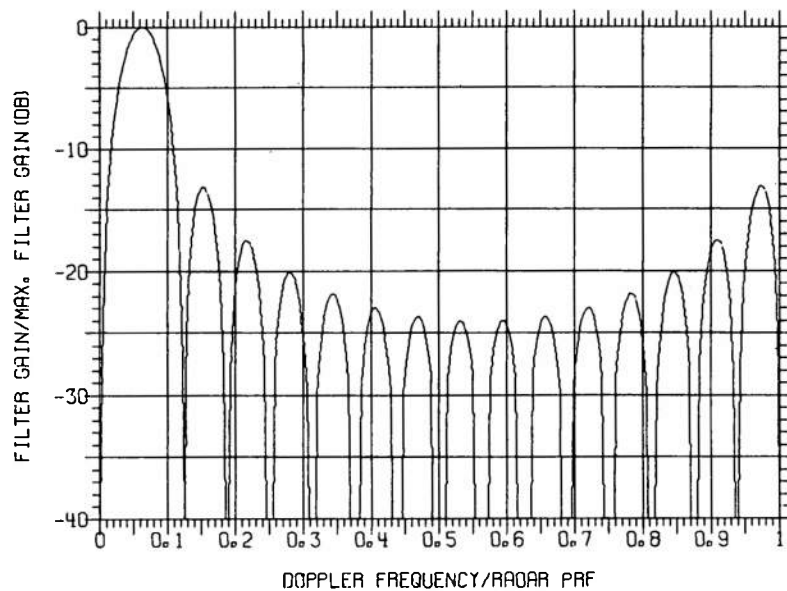
These filters have a  $(\sin x)/x$  shape and are translated in frequency by the index  $k$ . When  $N = 16$ , the filter responses for  $k = 1$  and  $k = 2$  are as shown in Figs. 6(a) and 6(b), respectively. The normalization used for these curves is

$$W_N = \sum_{n=1}^N |W_{kn}|^2 = 256$$

for  $N = 16$ .



(a)



(b)

Fig. 6 — Normalized power transfer function (filter response) for (a) filter no. 1 and (b) filter no. 2 of a 16-pulse (16-filter) MTI integrator

*Improvement Factor* — The improvement factor for the coherent integration is computed the same way as for the MTI discussed in Section III. Equation (13) is used with the weight vector  $W$  generated by Eq. (15). The signal covariance matrix  $M_s$  is generated using Eq. (12), with the bandwidth  $B$  given by

$$B = \frac{1}{N}$$

where  $N$  is the number of pulses integrated. The center of the  $i$ th filter,  $f_i$ , is given by

$$f_i = \frac{i-1}{N}, i = 1, 2, \dots, N.$$

The improvement factor is shown in Fig. 7(a) for an 8-pulse integrator and in Fig. 7(b) for a 16-pulse integrator. The gains of the filters are averaged and shown by a dotted curve in each figure. The average gain corresponds to the expected improvement factor for a target with equal probability of occurring in any filter. This average improvement factor should be compared with the MTI improvement factor shown in Fig. 5, which was computed for a target with equal probability of occurring at any doppler.

The irregularities in Fig. 7 are caused by the interaction between the clutter spectrum and the filter transfer function. Note that the width of the sidelobes of the filters, as shown in Fig. 6, is given by  $\text{PRF}/N$ , i.e., by  $0.125 \times \text{PRF}$  for an 8-pulse integrator and by  $0.0625 \times \text{PRF}$  for a 16-pulse integrator. At the left side of Fig. 7 the clutter spectrum is narrow as compared to the sidelobe width so that more of the clutter energy coincides with the null between sidelobes. The improvement factor is reduced as the clutter width is increased and more energy coincides with a peak in the sidelobes. This effect continues until the clutter width becomes wide enough for an appreciable amount of clutter energy to coincide with the next sidelobe null. In this region, less clutter energy is passed, and the improvement factor decreases at a slower rate as the clutter spectral width is increased. This effect continues until an appreciable amount of clutter energy coincides with the next peak in the sidelobes.

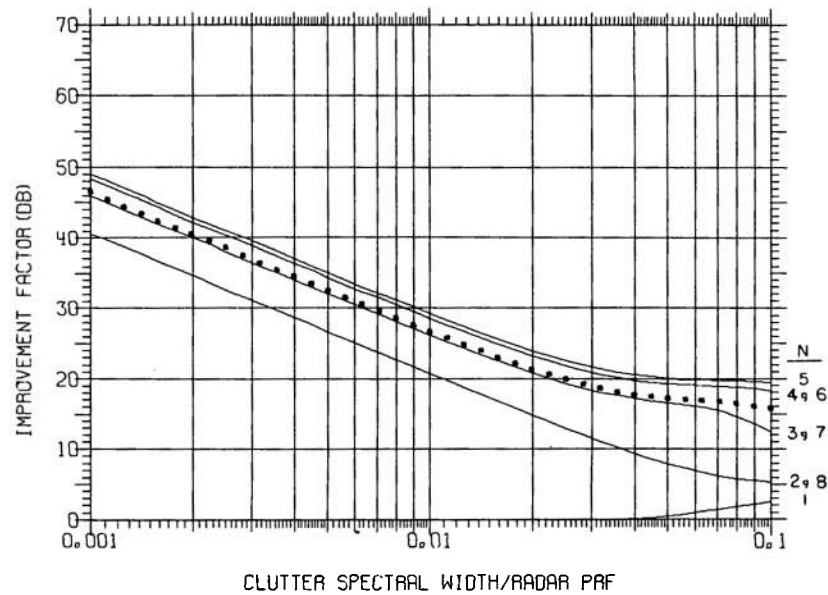
For narrow clutter spectral widths, the improvement factors for the 8- and 16-pulse integrators are approximately the same, as can be seen in Figs. 7 (a) and (b). Intuition would seem to indicate that the integration of more pulses should result in more gain in the signal-to-clutter ratio. When the interference consists of "white" noise, the improvement  $I$  in signal-to-noise ratio is given by

$$I = 10 \log N$$

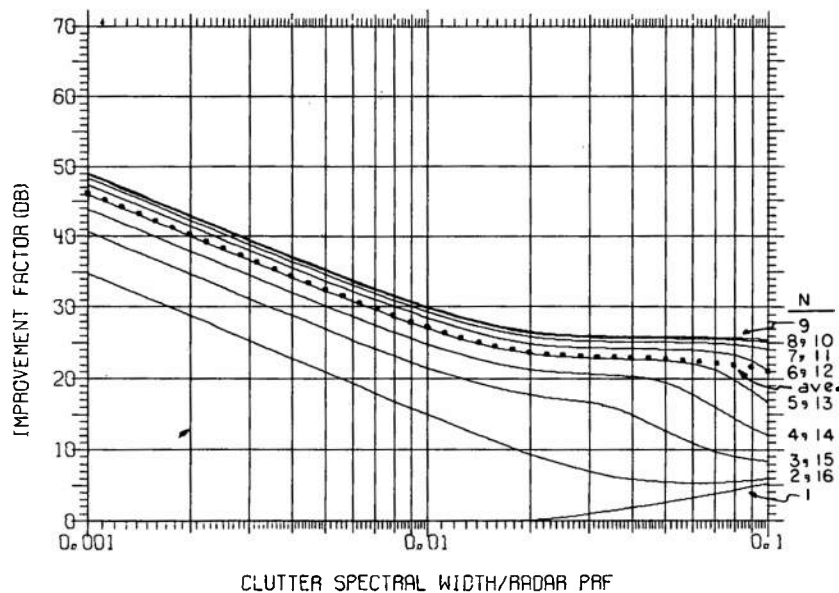
which, as expected, does give a larger improvement as  $N$  is increased.

For correlated (or "colored") noise, the gain that can be realized depends on the shape of the noise spectrum and the shape of the filter transfer function. Except for filter number one, all the filters generated by both the 8- and 16-pulse integrators have sidelobe nulls at zero doppler. The width of the null for an 8-pulse integrator is twice as wide as for a 16-pulse integrator. Apparently, the additional clutter rejection caused by the wider null of the 8-pulse integrator offsets the additional integration gain of the 16-pulse integrator.





(a)



(b)

Fig. 7 — Improvement factor  $I$  [given by Eq. (13)] for the indicated filter number  $N$  in (a) an 8-pulse and (b) a 16-pulse coherent integrator with uniform weighting. The average improvement for all filters is indicated by the dotted curve.

For wide clutter spectral widths, this effect disappears and the 16-pulse integrator achieves more gain. The wider spectral width is more characteristic of "white" noise.

Notice that filter number one has its mainlobe at zero doppler, as shown in Fig. 6(a). The clutter spectrum is also centered at zero doppler. For these reasons, the improvement factor for filter number one, as shown in Fig. 7, increases as the clutter spectral width increases since this results in more clutter energy outside the filter mainlobe region.

### Tschebyschev Weights

The sidelobes levels of the filters shown in Fig. 6 can be reduced by using a data "window" function (Ref. 8). This corresponds to weighting the input time samples  $x_n$  of Eq. (14). Let  $x_n \rightarrow a_n x_n$  in Eq. (14) where  $a_n$  is the weight vector for a desired filter shape. Then, from Eq. (15), the total effective weights of the  $k$ th filter become

$$W_{kn} = a_n e^{-j2\pi \frac{(n-1)(k-1)}{N}}, \quad n = 1, 2, \dots, N. \quad (16)$$

When the weights  $a_n$  correspond to the familiar Tschebyschev weights for a -25 dB sidelobe level, a 16-pulse coherent integrator results in 16 filters, two of which are shown in Figs. 8(a) and (b).

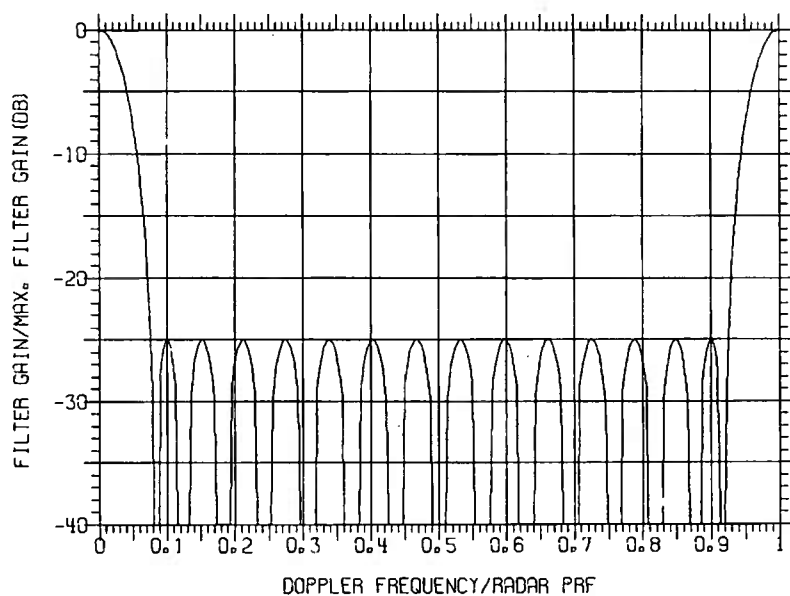
*Improvement Factor* — The improvement factors for 8- and 16-pulse integrators with -25 dB sidelobes are shown in Figs. 9(a) and 9(b), respectively. Notice that at narrow clutter spectral widths, the average improvement factor of the 8-pulse integrator is greater than the average improvement of the 16-pulse integrator. Also, notice the irregular ordering of the filters in Fig. 9(b) for narrow clutter spectral widths. Those filters whose center frequencies are farther from the clutter spectrum center (zero doppler) might be expected to have a higher improvement factor than filters nearer to the clutter. However, for a narrow clutter spectrum, this does not happen. These peculiarities are a result of the irregular sidelobe and null widths produced by the Tschebyschev weighting. A filter that is closer to the clutter may have a wider null near zero doppler and, therefore, realize a higher improvement factor.

An examination of Figs. 7 and 9 reveals a certain degree of unpredictability for coherent integration filters in a clutter (or "colored" noise) environment. This unpredictability could be reduced by preceding the integration filters with a "clutter" filter, such as an MTI canceller, to reduce the coherency of the clutter input to the integration filters. This configuration will be examined in the following section.

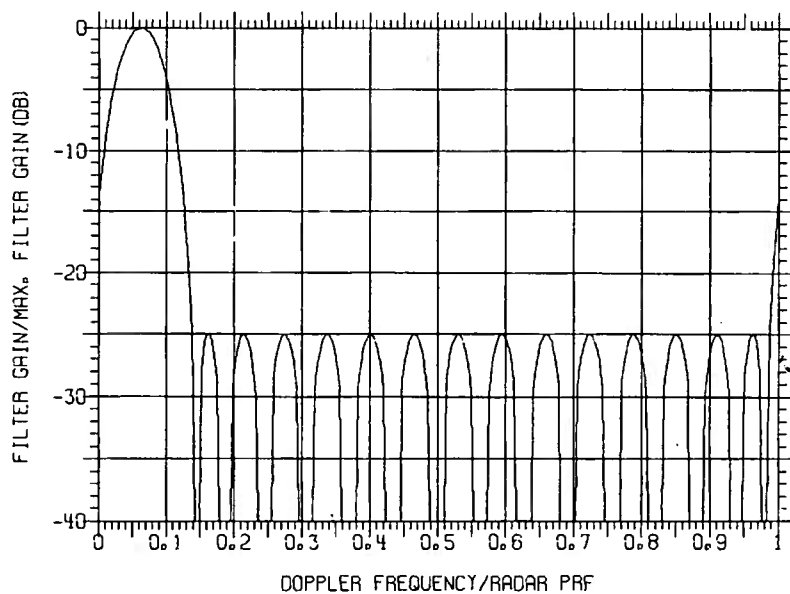
## V. CASCADED MTI AND COHERENT INTEGRATOR

### Optimum Cascaded Filters

The maximum improvement in signal-to-clutter ratio could be achieved by following a "prewhitening" filter with a filter matched to the target return. Since the target doppler spectrum considered by this report is a single line component, the matched filter cannot

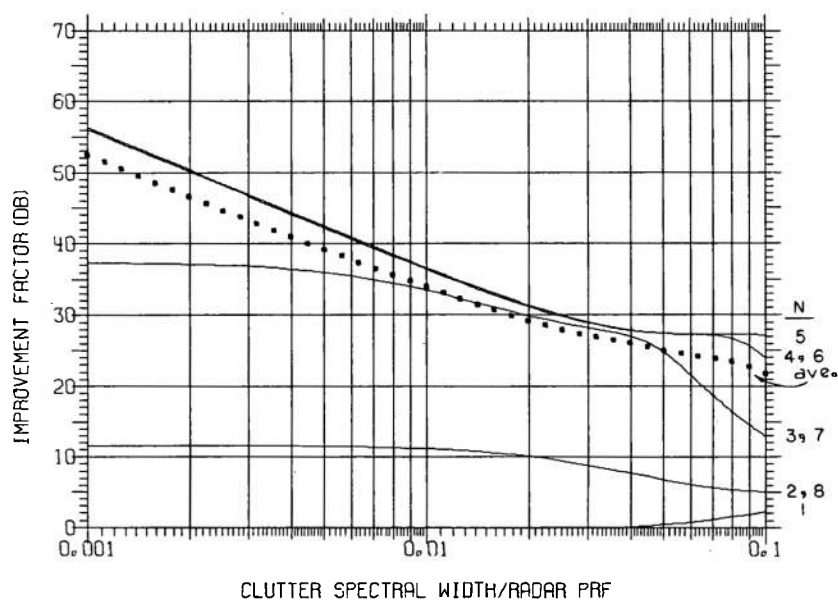


(a)

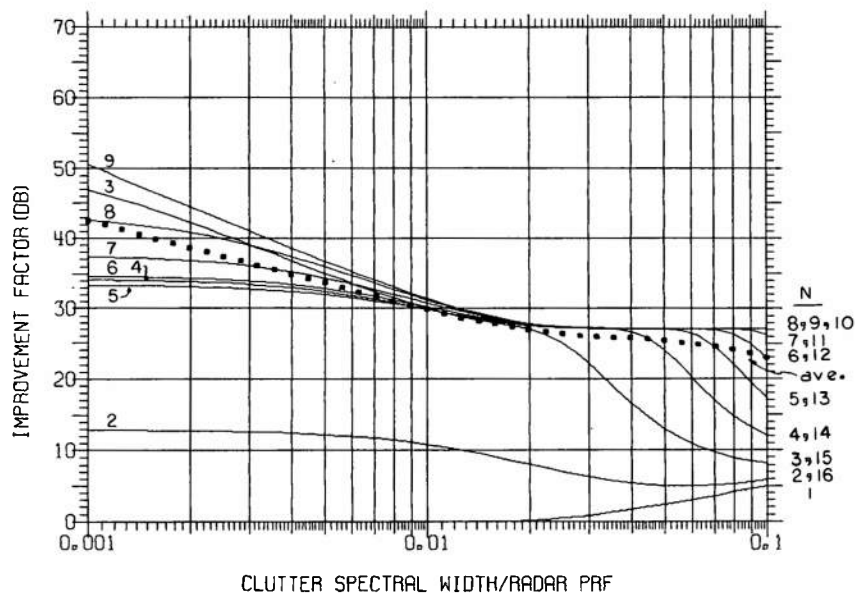


(b)

Fig. 8 — Normalized power transfer function (filter response) for (a) filter no. 1 and (b) filter no. 2 in a 16-pulse coherent integrator. The input time samples  $x_n$  are Tschebyshev weighted for a -25 dB side-lobe level. (Compare with Fig. 6.)



(a)



(b)

Fig. 9 — Improvement factor  $I$  [given by Eq. (13)] for (a) an 8-pulse and (b) a 16-pulse coherent integrator with Tschebyshev weighting. The average improvement for all filters is indicated by the dotted curve.

be realized by a processor with a finite processing time. However, the coherent integration filters considered in the previous section are an approximation to a matched filter. The approximation is limited only by the processing time (or the number of pulses integrated).

To completely "prewhiten" the clutter prior to coherent integration, the prewhitening filter must have a processing time equal to the processing time of the coherent integrator, i.e. each filter must process the same number of pulses. Although this approach gives the classical matched filter in "colored" noise, and therefore gives the maximum improvement in signal-to-clutter ratio, it is worthwhile to consider substituting for the ideal prewhitening filter a more simple filter with a shorter processing time. Any clutter notch filter that precedes the integration filters reduces the dynamic range of the input to the integration filters by an amount equal to the clutter rejection realized by the clutter notch. This requires less storage for the integration filters.

In this report, the three clutter notch filters considered are MTIs consisting of (a) a single canceller, (b) a double canceller, and (c) a triple canceller. The integration filters considered are an 8- and a 16-pulse FFT. Therefore, the processing time of the clutter filter is less than the processing time of the integration filter.

Some care is required in the analysis of a cascaded combination of two sampled data filters with different processing times. Theoretically, the order of the filters can be interchanged with the same results since both filters are linear. For analysis it is convenient to consider the filter with the shorter processing time first, and then the filter with the longer processing time. Also, for practical reasons, the MTI should precede the integration filter to reduce the dynamic range that the integration filter has to handle.

### Matrix Equations For Cascaded Filters

To analyze the cascaded filters in terms of the matrix operation of the preceding sections, consider the filter arrangement shown in Fig. 10. The first filter is characterized by the number  $M$  of pulses processed and by the weight vector  $A$ . The second filter is characterized by the number  $N$  of pulses it processes and by its weight vector  $B$ . The number  $M$  is always less than  $N$ .

The output  $z(t)$  of these filters can be expressed in terms of the input  $y(t)$  to the second filter by means of the matrix equation

$$z = B_T Y \quad (17)$$

where

$$Y = \begin{bmatrix} y_1 \\ y_2 \\ \cdot \\ \cdot \\ y_N \end{bmatrix} \quad \text{and} \quad B = \begin{bmatrix} b_1 \\ b_2 \\ \cdot \\ \cdot \\ b_N \end{bmatrix}$$

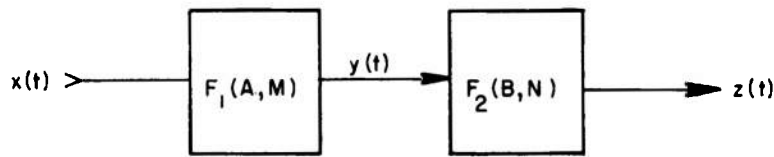


Fig. 10 — Cascaded filters with different processing times.  $M$  and  $N$  are the number of pulses processed ( $M < N$ ), and  $A$  and  $B$  are weight vectors.

with  $B_T$  being the transpose of the weight vector  $B$ . The components of  $Y$  can be related to the input  $x(t)$  by

$$\begin{aligned} y_1 &= a_1 x_1 + a_2 x_2 + \dots + a_M x_M \\ y_2 &= a_1 x_2 + a_2 x_3 + \dots + a_M x_{M+1} \\ &\vdots \\ y_N &= a_1 x_N + a_2 x_{N+1} + \dots + a_M x_{M+N-1}. \end{aligned}$$

Let

$$X = \begin{bmatrix} x_1 \\ x_2 \\ \vdots \\ x_{M+N-1} \end{bmatrix} \quad \text{and} \quad A_1 = \begin{bmatrix} a_1 \\ a_2 \\ \vdots \\ a_M \\ 0 \\ 0 \\ \vdots \\ \vdots \\ \vdots \end{bmatrix} \quad \left. \begin{array}{c} \\ \\ \\ \\ 0 \\ 0 \\ \vdots \\ \vdots \\ \vdots \end{array} \right\} \begin{array}{l} \\ \\ \\ \\ N-1 \text{ zeros} \end{array}$$

Then

$$y_1 = (A_1)_T X.$$

In the same way

$$y_2 = (A_2)_T X,$$

where

$$A_2 = \begin{bmatrix} 0 \\ a_1 \\ a_2 \\ \vdots \\ \vdots \\ \vdots \\ a_M \\ 0 \\ 0 \\ \vdots \\ \vdots \\ \vdots \end{bmatrix} \left. \begin{array}{l} \text{1 zero} \\ \\ \\ \\ \\ \\ \\ \text{N-2 zeros} \end{array} \right\} ,$$

and

$$y_N = (A_N)_T X$$

where

$$A_N = \begin{bmatrix} 0 \\ 0 \\ \vdots \\ \vdots \\ \vdots \\ a_1 \\ a_2 \\ \vdots \\ \vdots \\ \vdots \\ a_M \end{bmatrix} \left. \begin{array}{l} \text{N-1 zeros} \end{array} \right\} .$$

Combining all of these matrix relations gives

$$Y = \hat{A}_T X \quad (19)$$

where  $X$  is given by Eq. (18) and

$$\hat{A} = [A_1 A_2 \dots A_N] .$$

Substituting Eq. (19) into Eq. (17), the matrix relationship between input and output becomes

$$\begin{aligned} z &= B_T \hat{A}_T X \\ &= W_T X \end{aligned} \quad (20)$$

since the total effective weight vector is given by

$$W = \hat{A}B. \quad (21)$$

Therefore this cascaded combination of filters can be evaluated in the same way that was outlined in section II and used in section III for the MTI filter and in section IV for the integration filter. The only difference is that the weight vector  $W$  is defined by Eq. (21) and generated as shown above.

### Transfer Function

The power transfer function of the cascaded filters can be computed by means of Eq. (7) and the weights given by Eq. (21). The signal covariance matrix  $M_s$  is generated from Eq. (12) by setting the bandwidth  $B$  equal to zero and varying the center frequency  $f_i$  from zero to  $1/T$ . The weight vector  $W$  is computed from Eq. (21), with the matrix  $\hat{A}$  generated from the weight vector  $A$  given by

$$A = \begin{bmatrix} a_1 \\ a_2 \\ \vdots \\ a_M \end{bmatrix}.$$

If the first filter is an MTI consisting of  $M - 1$  binomial cancellers, then

$$a_i = (-1)^{i-1} \binom{M-1}{i-1}, \quad i = 1, 2, \dots, M \quad (22)$$

as shown in section III. If the second filter is an FFT with uniform weights, then the weight vector  $B$  can be generated from Eq. (15).

Using this procedure, the power transfer functions generated by a triple-canceller MTI cascaded with a 16-pulse coherent integrator are shown in Figs. 11(a)-(i) for nine of the sixteen filters. Filter no. 10 is the mirror image of filter no. 8; filter no. 11 is the mirror image of filter no. 7, etc. Uniform integrator weights are used. When 25-dB Tschebyshev weights are used, the resulting transfer functions are shown in Figs. 12(a)-(i). The filter patterns are analogous to the antenna patterns obtained with a 16-element linear array with elements equally spaced at one-half wavelength. The element pattern is analogous to the MTI filter transfer function. All filter transfer functions are normalized to the maximum gain of the center filter (filter no.  $(N/2) + 1$ , where  $N$  is the number of pulses integrated).

### Improvement Factor

The improvement in signal-to-clutter ratio is shown in Figs. 13(a) and (b) for a single canceller cascaded with an 8-pulse integrator. With 25-dB Tschebyshev weights [Fig. 13(b)] there is a larger variation in gain between filters. However, the average gain is greater by 5 to 6 dB than for uniform weights [Fig. 13(a)]. The integrator with uniform weights has more



gain in the filters near the clutter spectrum, i.e., filters no. 2 and 8. The MTI null at zero doppler overrides the gain that was achieved by filter no. 1 without MTI.

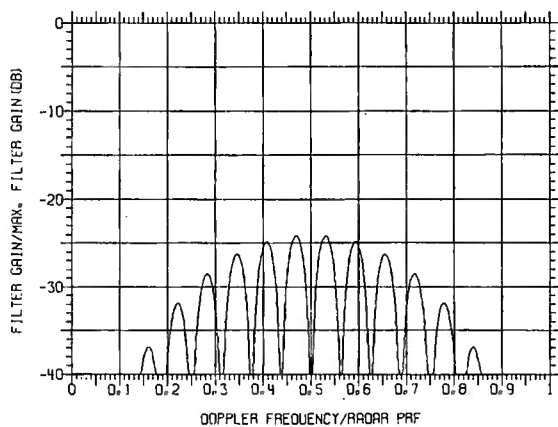
Figures 14(a) and (b) show the improvement factors for a single canceller cascaded with a 16-pulse integrator. Again, with 25-dB Tschebyshev weights [Fig. 14(b)] there is a larger variation in gain between filters. The filters near the clutter spectrum again have less gain than the same filters with uniform weights [Fig. 14(a)]. However, the average filter gain is slightly higher (about 3 dB), for narrow clutter spectral widths ( $0.001 \times \text{PRF}$ ) using uniform weights, but slightly higher (about 2 dB) for wide clutter widths ( $0.1 \times \text{PRF}$ ) using 25-dB weights. Comparing Figs. 13 and 14 shows that the average improvement factor is still less for a 16-pulse integrator than for an 8-pulse integrator for narrow clutter. This effect was noticed for the 8- and 16-pulse integrators without MTI.

Figures 15(a) and (b) show the improvement factors for a double canceller cascaded with an 8-pulse integrator. The characteristics of these curves are similar to Fig. 13 for a single canceller and an 8-pulse integrator. With 25-dB weights [Fig. 15(b)] there is a larger variation in filter gains, but also a larger (again 5 to 6 dB) average filter gain. The additional improvement factor realized by preceding an 8-pulse integrator with a double canceller (Fig. 15) instead of with a single canceller (Fig. 13) varies from 42 dB for narrow clutter widths ( $0.001 \times \text{PRF}$ ) to 4 dB for wide clutter widths ( $0.1 \times \text{PRF}$ ) using either uniform or 25-dB weights.

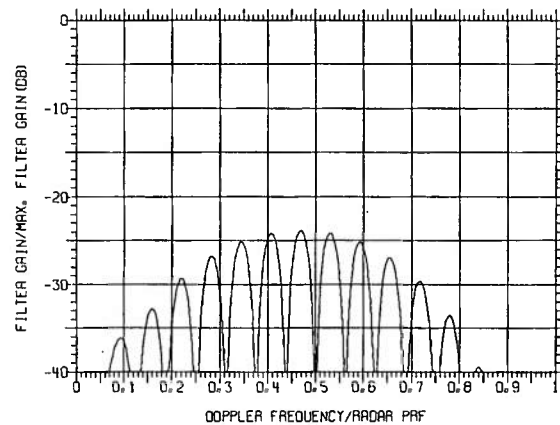
Figures 16(a) and (b) show the improvement factor for a double canceller cascaded with a 16-pulse integrator. Comparing uniform weights [Fig. 16(a)] with 25-dB weights [Fig. 16(b)], the difference in the variation in filter gain is reduced, although the filters near the clutter spectrum still have less gain with 25-dB weights for narrow clutter. For narrow clutter widths, uniform weights give about 2 dB more average gain. For wide clutter widths, 25-dB weights give about 2 dB more average gain. The additional improvement factor realized by preceding a 16-pulse integrator with a double canceller (Fig. 16) instead of with a single canceller (Fig. 14) varies from about 42 dB for narrow clutter to about 4 dB for wide clutter using either uniform or 25-dB weights. This is the same improvement that was achieved by preceding the 8-pulse integrator with a double instead of with a single canceller.

Figures 17(a) and (b) show the improvement factor for a triple canceller cascaded with an 8-pulse integrator. Comparing uniform weights [Fig. 17(a)] with 25-dB weights [Fig. 17(b)], the 25-dB weights still cause a wider variation in filter gains, with the filters near the clutter having appreciably less gain than the same filters with uniform weights. The average gain is always greater with 25-dB weights, varying from about 6 dB with narrow clutter to about 4 dB for wide clutter. The additional improvement factor realized by preceding an 8-pulse integrator with a triple canceller (Fig. 17) instead of with a double canceller (Fig. 15) varies from more than 30 dB for narrow clutter to about 3 dB for wide clutter using uniform weights, and varies from more than 30 dB to about 2 dB using 25-dB weights.

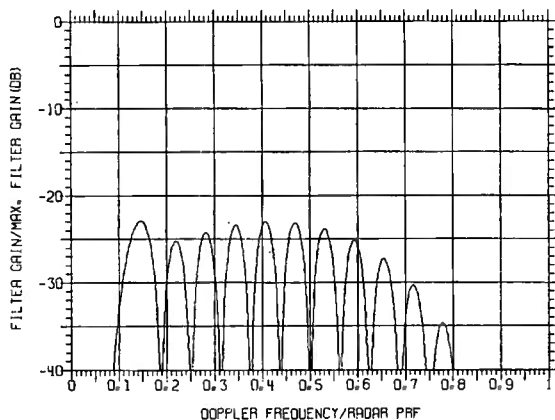
Figures 18(a) and (b) show the improvement factor for a triple canceller cascaded with a 16-pulse integrator. Again, the 25-dB weights cause a wider variation in filter gains. The average filter gain is always about 2 dB greater for 25-dB weights. The additional improvement realized by preceding the 16-pulse integrator with a triple canceller (Fig. 18) instead of with a double canceller (Fig. 16) varies from more than 30 dB for narrow clutter to about 3 dB for wide clutter. This is the same increase that was achieved by preceding the 8-pulse integrator with a triple canceller instead of with a double canceller.



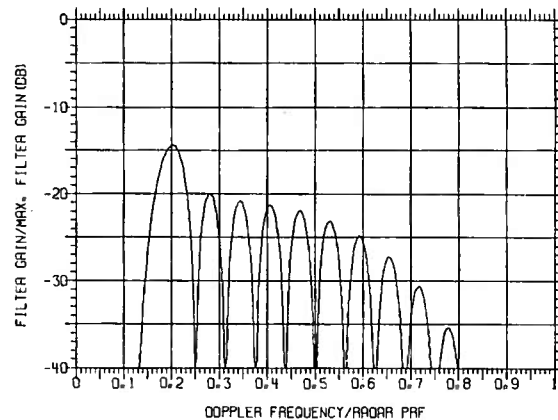
(a)



(b)

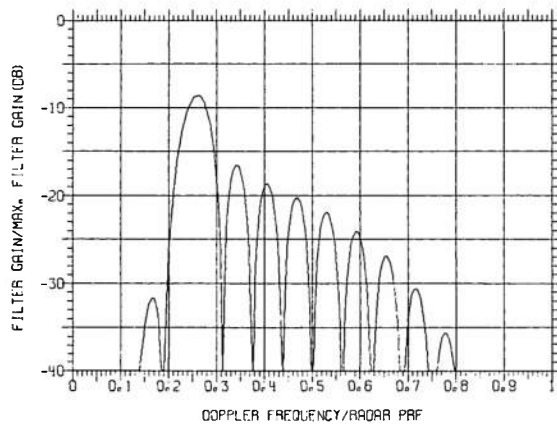


(c)

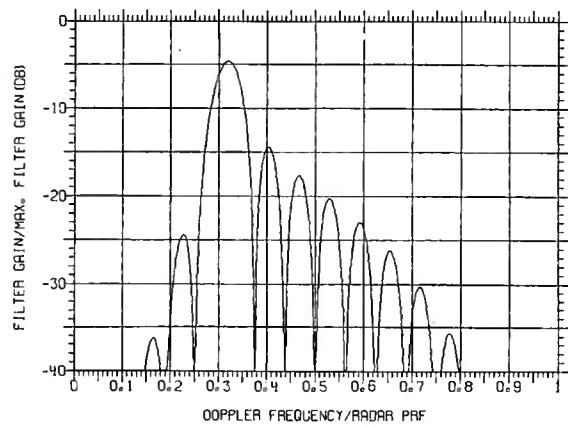


(d)

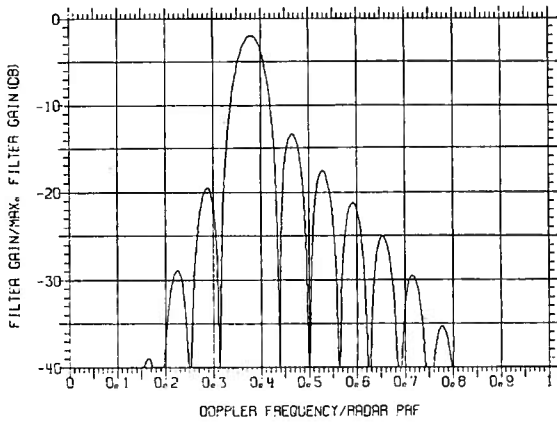
Fig. 11 — Normalized power transfer function for a triple-canceller MTI cascaded with a 16-pulse coherent integrator. The transfer functions for nine of the sixteen filters (filters no. 1 through 9) are shown in the graphs labeled (a) through (i). The integrator filters have been uniformly weighted.



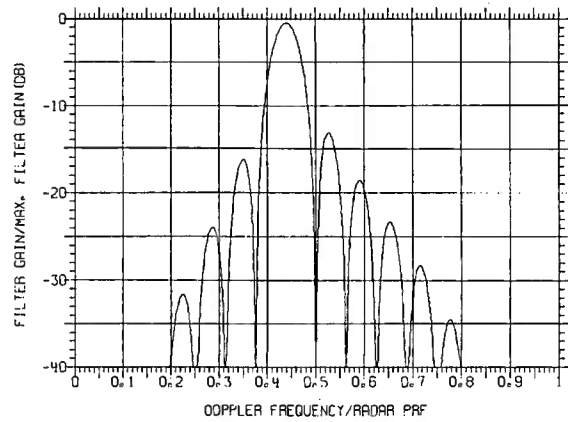
(e)



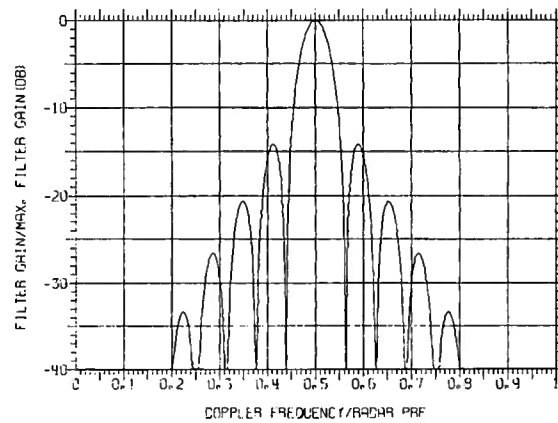
(f)



(g)



(h)



(i)

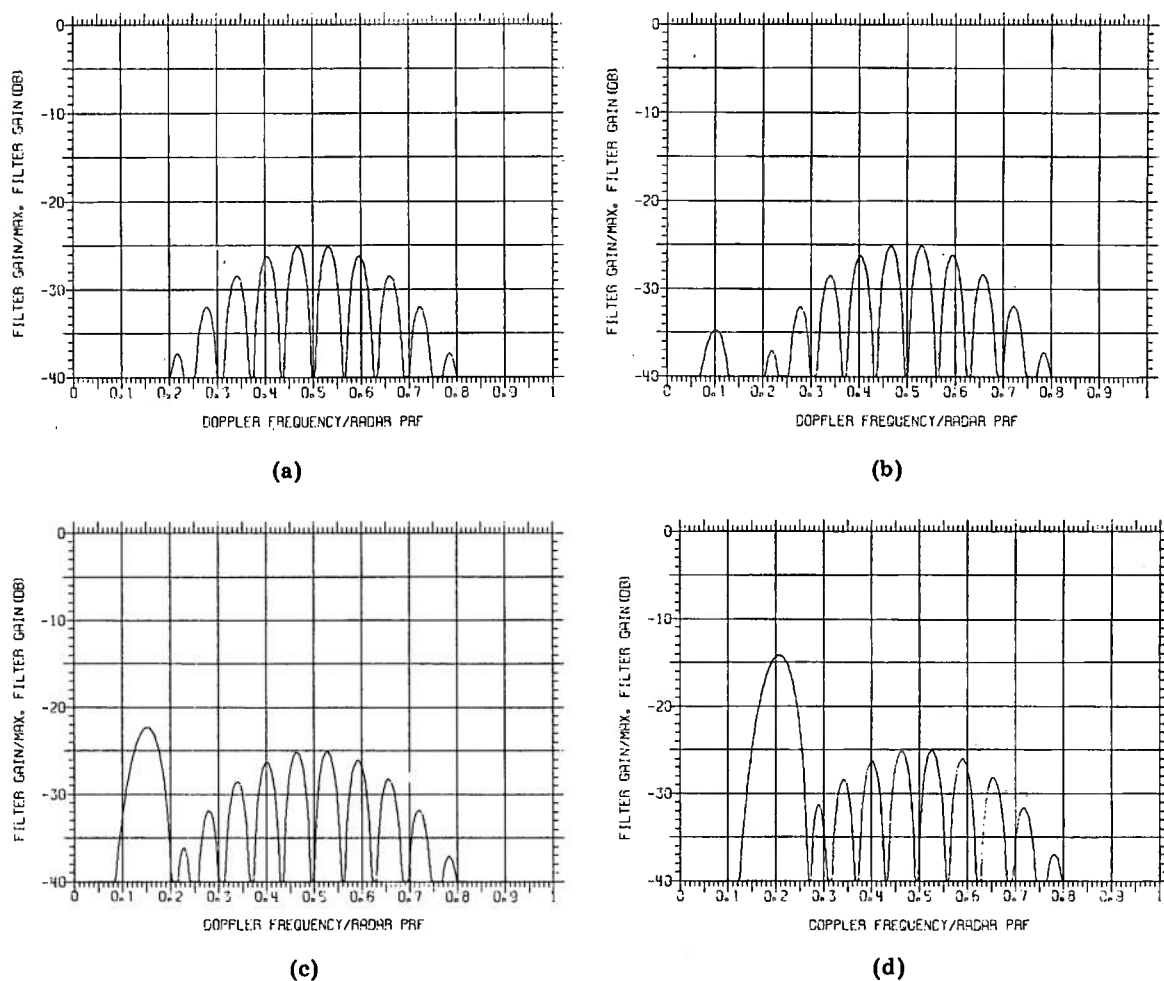
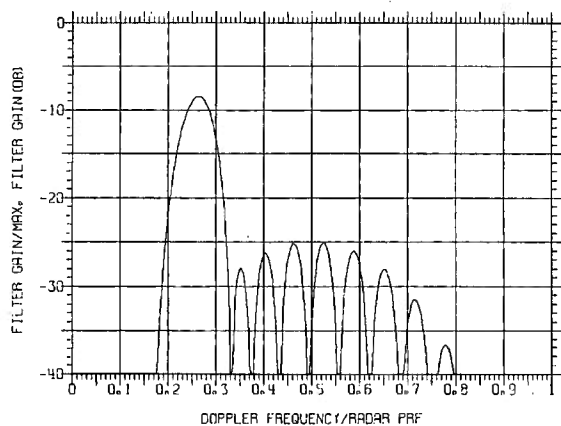
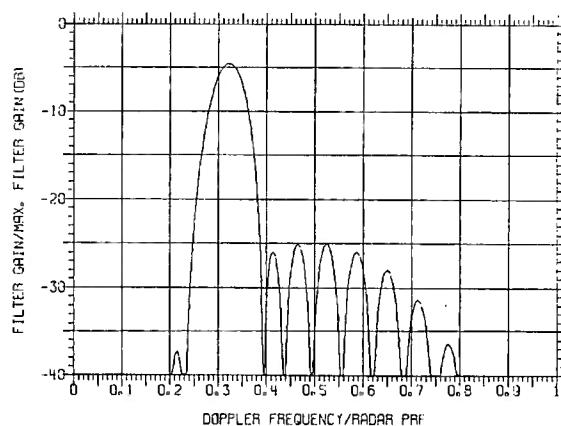


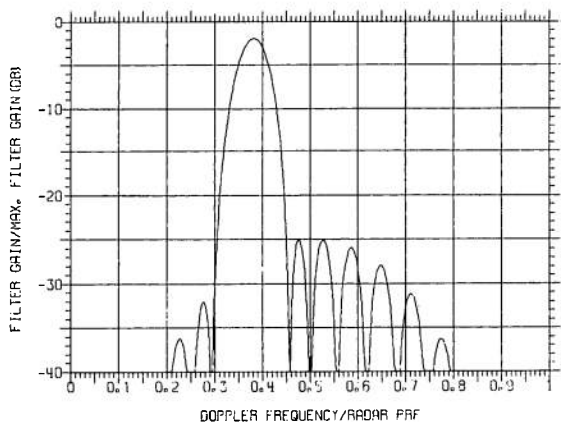
Fig. 12 — Normalized power transfer function for a triple-canceller MTI cascaded with a 16-pulse coherent integrator. The transfer functions for nine of the sixteen filters (filters no. 1 through 9) are shown in the graphs labeled (a) through (i). The integrator filters have been Tschebyschev weighted for a -25 dB sidelobe level (Compare with Fig. 11.)



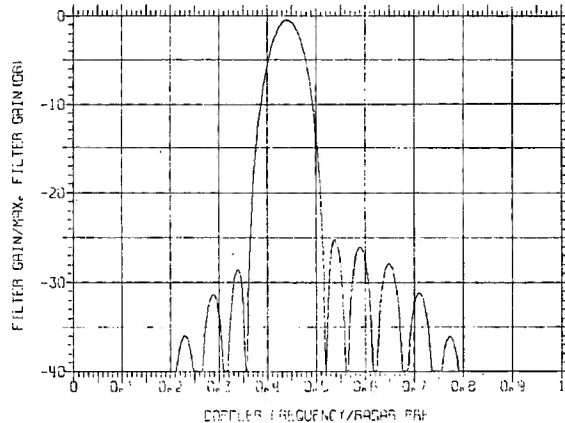
(e)



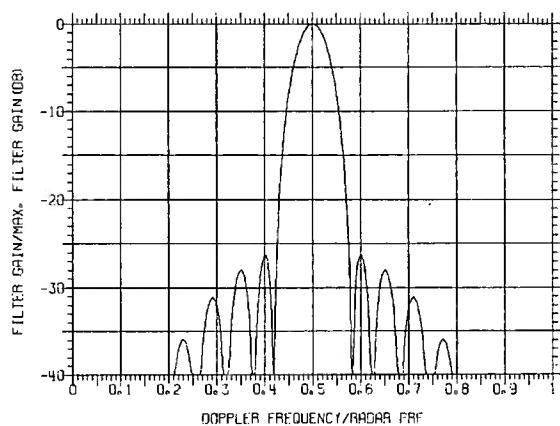
(f)



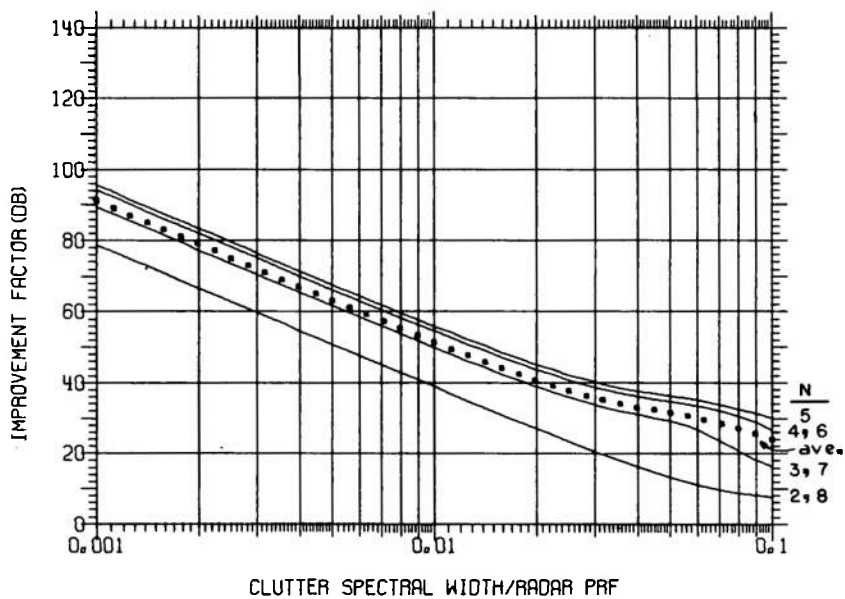
(g)



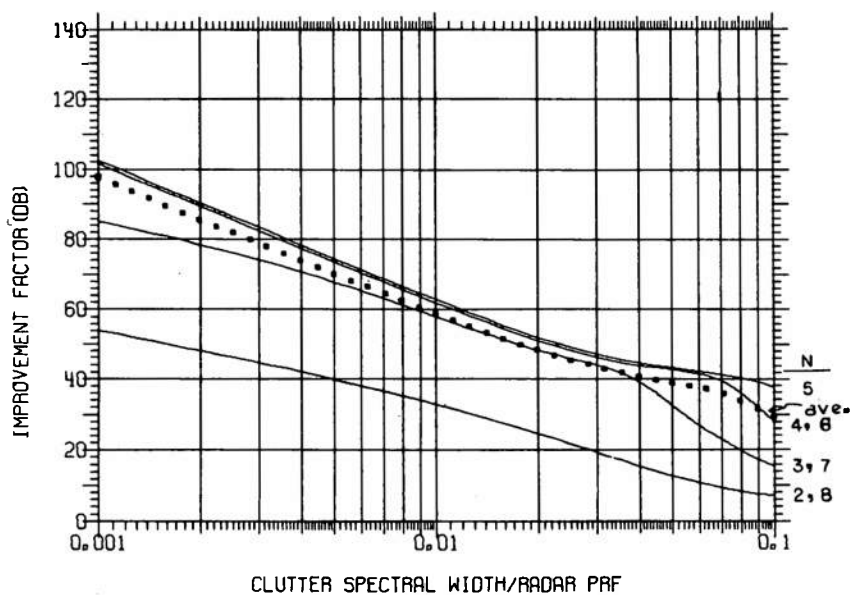
(h)



(i)

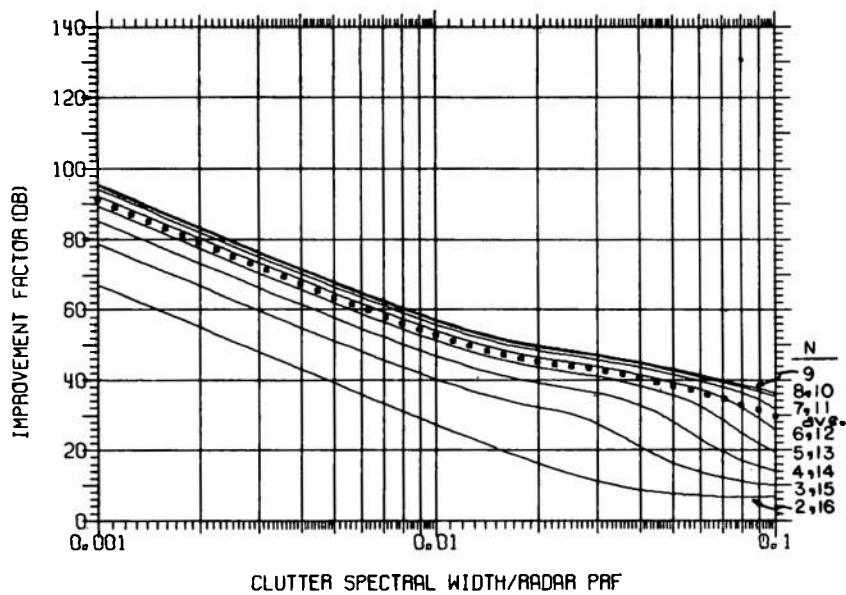


(a)

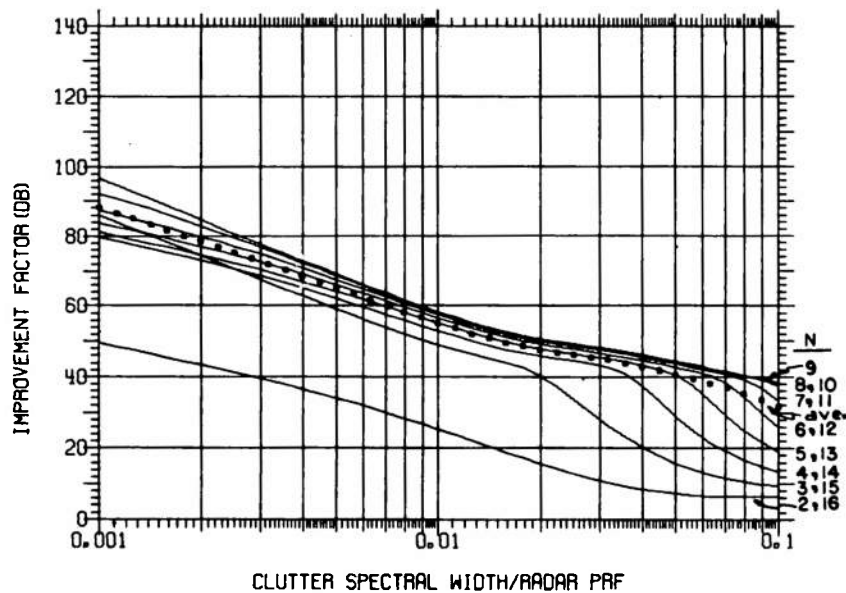


(b)

Fig. 13 — Improvement factor  $I$  [given by Eq. (13)] for a single-canceller MTI cascaded with an 8-pulse integrator. The integrator filters have been (a) uniformly weighted and (b) 25-dB Tschhebyshev weighted. The average improvement for all filters is indicated by the dotted curve.

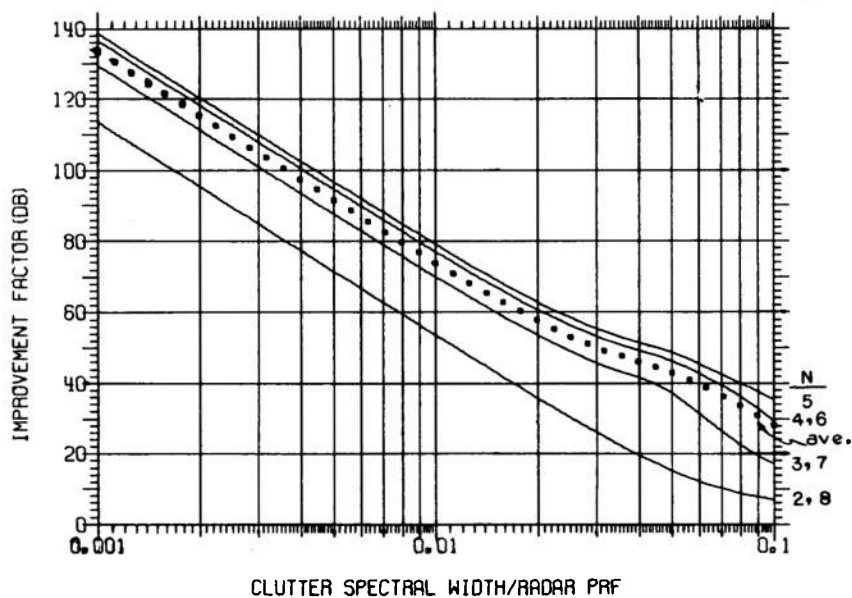


(a)

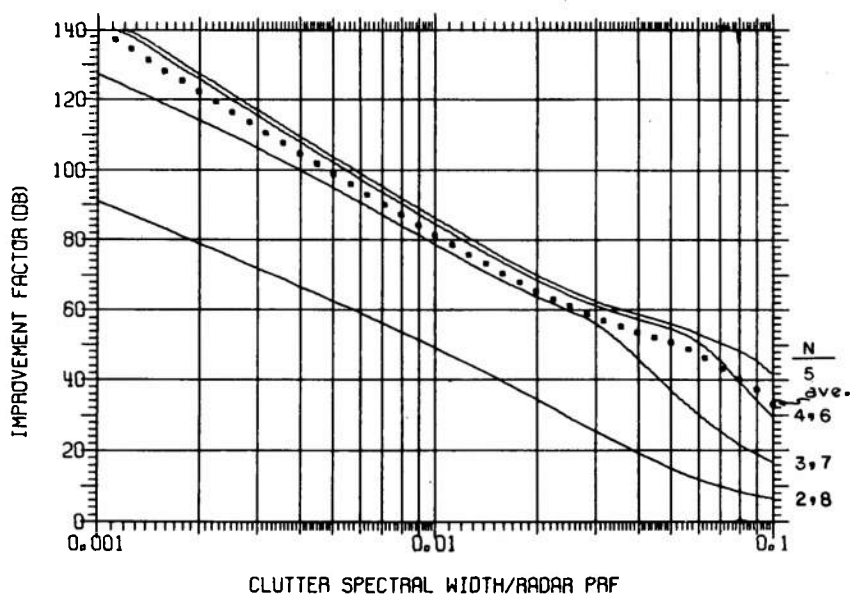


(b)

Fig. 14 — Improvement factor  $I$  [given by Eq. (13)] for a single-canceller MTI cascaded with a 16-pulse integrator. The integrator filters have been (a) uniformly weighted and (b) 25-dB Tchebyshev weighted. The average improvement for all filters is indicated by the dotted curve.



(a)



(b)

Fig. 15 — Improvement factor  $I$  [given by Eq. (13)] for a double-canceller MTI cascaded with an 8-pulse integrator. The integrator filters have been (a) uniformly weighted and (b) 25-dB Tschhebyshev weighted. The average improvement for all filters is indicated by the dotted curve. (Compare with Fig. 13.)



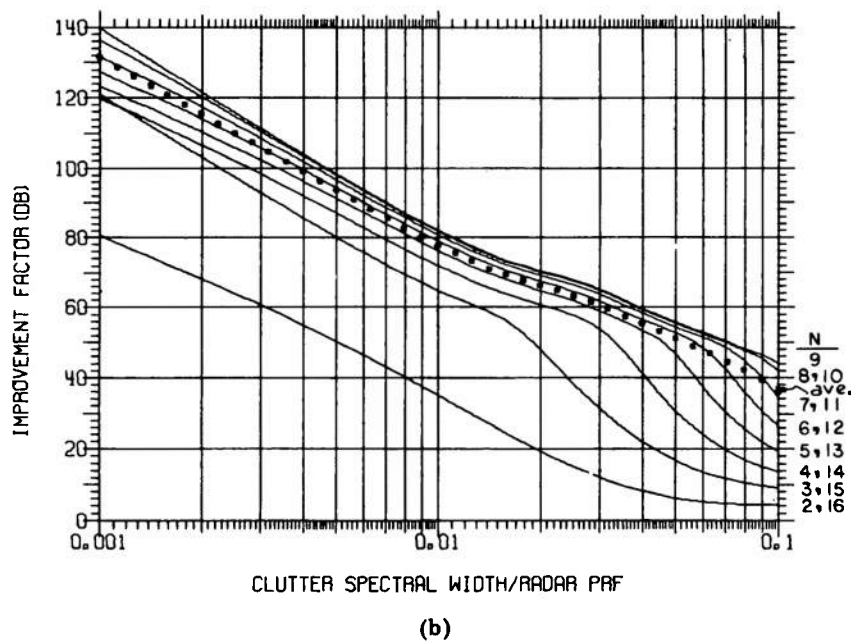
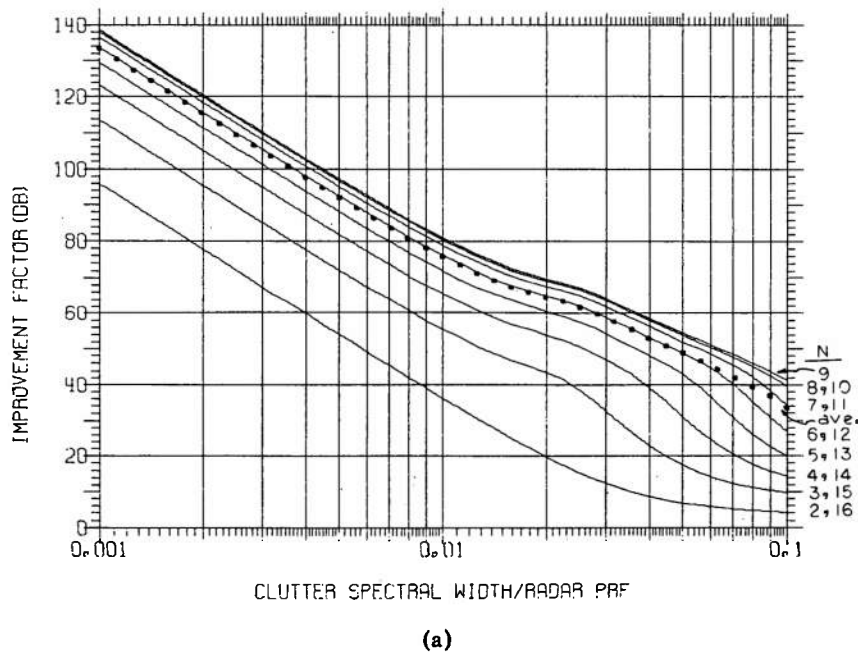


Fig. 16 — Improvement factor  $I$  [given by Eq. (13)] for a double-canceller MTI cascaded with a 16-pulse integrator. The integrator filters have been (a) uniformly weighted and (b) 25-dB Tschebyshev weighted. The average improvement for all filters is indicated by the dotted curve. (Compare with Fig. 14.)

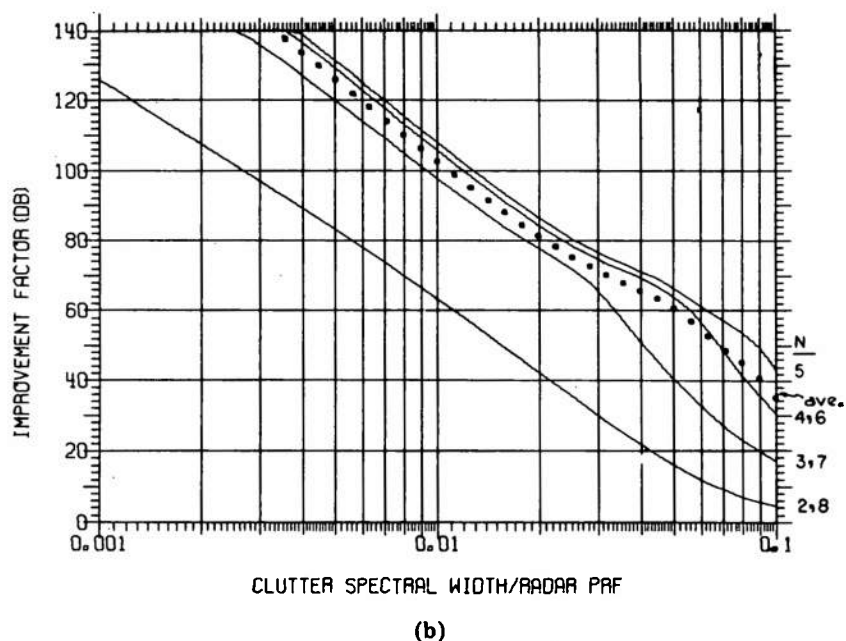
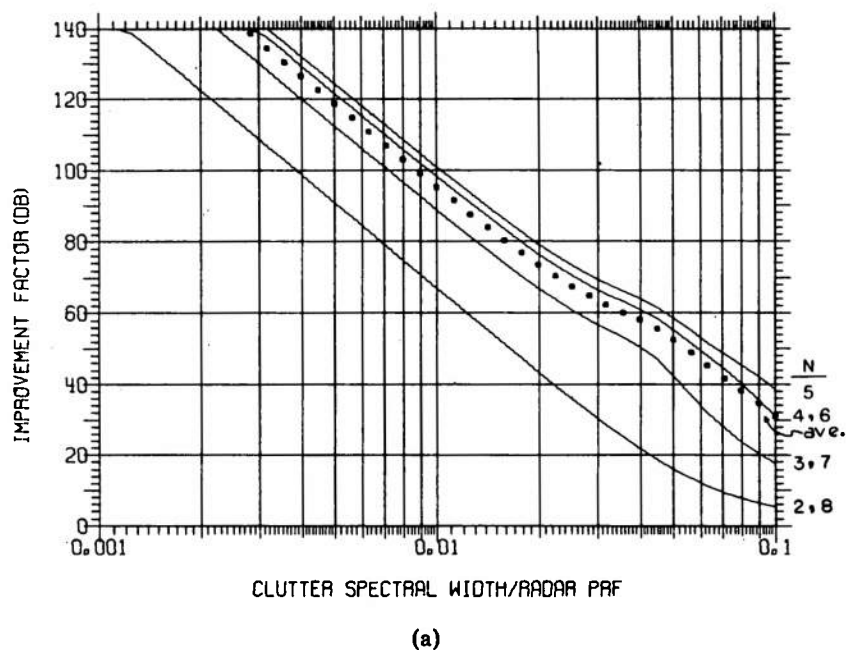


Fig. 17 — Improvement factor  $I$  [given by Eq. (13)] for a triple-canceller MTI cascaded with an 8-pulse integrator. The integrator filters have been (a) uniformly weighted and (b) 25-dB Tschebyshev weighted. The average improvement for all filters is indicated by the dotted curve. (Compare with Fig. 15.)

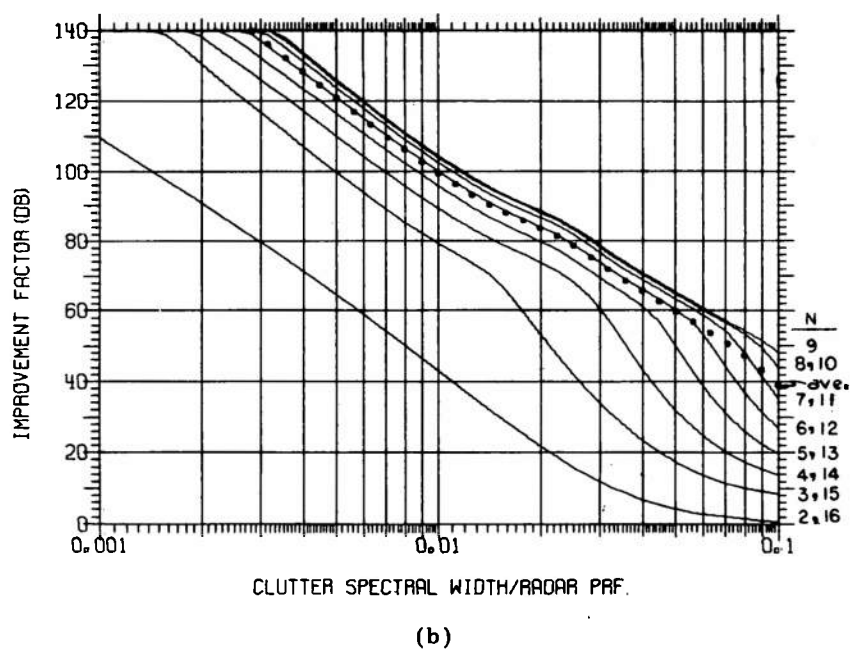
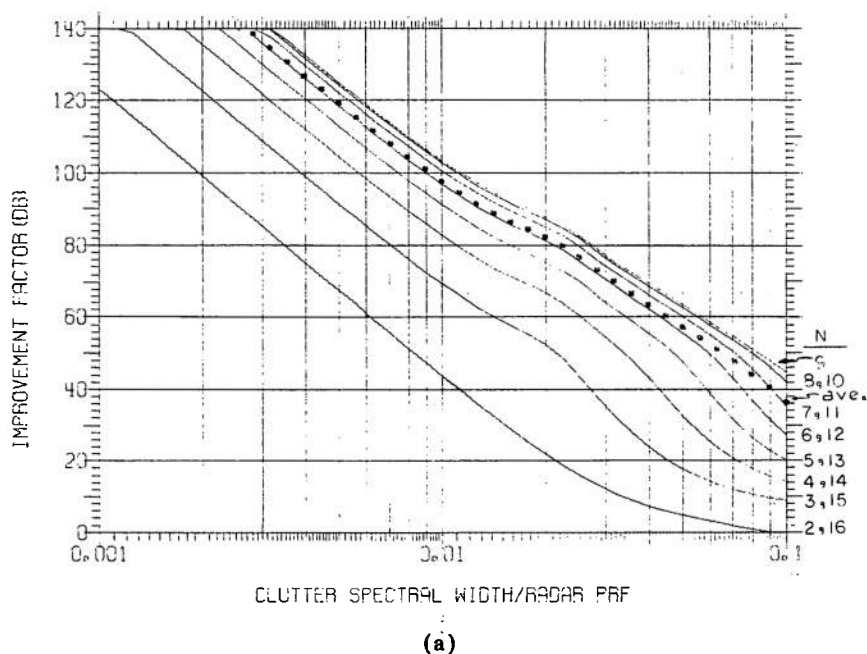


Fig. 18 — Improvement factor  $I$  [given by Eq. (13)] for a triple-canceller MTI cascaded with a 16-pulse integrator. The integrator filters have been (a) uniformly weighted and (b) 25-dB Tschebyshev weighted. The average improvement for all filters is indicated by the dotted curve. (Compare with Fig. 16.)

## VI. CONCLUSIONS

Coherent integration is a technique that has been used in radar systems to improve detection in a "white" noise (i.e., receiver noise) environment and also to reject clutter in high-PRF radars. More recently this technique has been considered for clutter rejection in low-PRF radars where the ratio of the clutter spectrum width to the PRF is much larger than for high-PRF systems. Less analysis is available for this application to aid in understanding and evaluating the performance of coherent integration.

This report has considered several particular doppler filters which consist of cascaded MTI and coherent integration filters. These filters are considered typical of the filters that would be applicable to a low-PRF radar which has a relatively small number of hits per dwell time. The computed improvement factors presented in Figs. 7, 9, and 13-18 show that coherent integration filters perform in an irregular, almost unpredictable, way when their input is "colored" noise (or clutter). The performance of coherent integrators against "white" noise is well established and easily predicted. Against "clutter", the performance is highly dependent upon the shape of the clutter spectrum and the shape (or weights) of the coherent integrator transfer functions. In particular, it is not necessarily true that more improvement is achieved by integrating more pulses for a given weight vector. On the other hand, it is theoretically true that weights exist which will allow more gain to be achieved when more pulses are processed. The computation of weight vectors that will give the maximum improvement in signal-to-clutter ratio under various optimization criteria will be presented in a later report.

The optimum weights obviously depend on the optimization criteria as well as on the shape of the interference spectrum. Of the integration filter weights discussed in the report, either uniform or 25-dB Tschebyshev weights could be selected as the "better" weights depending on the criterion used. This is pointed out by the following specific results:

- a. 25-dB Tschebyshev weights give more average gain than uniform weights.
- b. Uniform weights generally give more gain in the filters near the clutter spectrum.
- c. Uniform weights result in less variation in gain from filter to filter.
- d. For very narrow clutter spectral widths, the integration of more pulses does not necessarily lead to more average gain.

These conclusions apply regardless of whether or not an MTI precedes the integrator. When an MTI is cascaded with the integrator, the following general conclusions can be made:

- a. The additional average gain achieved by cascading an MTI with any particular integrator is only very slightly affected by the type of integrator. That is, cascading a single canceller with an 8-pulse integrator results in about the same additional gain above an 8-pulse integrator alone as the additional gain above a 16-pulse integrator achieved by cascading a single canceller with a 16-pulse integrator. [Compare Fig. 7(a) with Fig. 13(a) and Fig. 7(b) with 14(a)]. An equivalent comparison can be made for double and triple cancellers.

b. The average gain achieved by cascading an integrator with any particular MTI is affected to some degree by the type of MTI. This can be seen by comparing the improvement factors for the MTI, shown in Fig. 5, with those in Figs. 13-18 for the MTI cascaded with integrators.

It might be concluded that the chief advantage of the coherent integrator lies not with its average performance in a clutter-dominated environment but with:

a. Increased gain for targets near the clutter spectrum. It narrows the "blind" velocity regions and could increase the detection of low-speed targets.

b. Increased gain in a "white" (i.e., receiver) noise environment. This also applies to other forms of wideband interference such as clutter received through the antenna sidelobes when the radar is on a moving platform. MTI alone has no capability against this type of interference.

c. Improved velocity measurement of targets for tracking or identification.

These factors must be considered in any tradeoff between cancellation and integration for a particular radar application and for a particular interference environment.

## VII. ACKNOWLEDGMENT

I would like to acknowledge the very special contributions to this effort by Mr. D. L. Ringwalt and Dr. T. L. ap Rhys through our many interesting discussions. I would also like to thank Mr. Benjamin Koo upon whose mathematical and programming advice this effort depended so heavily. Finally, I would like to thank Mrs. Rosalie Valentine and Mrs. Evelyn Starrett for their determination in typing from a barely legible manuscript.

## VIII. REFERENCES

1. Skolnik, M.I., ed., "Radar Handbook," New York:McGraw-Hill, 1970.
2. McAulay, R.J., "A Theory for Optimal MTI Digital Signal Processing," Tech. Note 1972-14, Lincoln Laboratory, Mass. Inst. of Tech., Lexington, Mass., Feb. 1972.
3. "Performance of a Cascaded Digital Canceller and Coherent Integrator," Report SR01-01, General Electric Company, Utica, NY, 13503, Mar. 1971.
4. "An AEW AMTI Technique for Obtaining Reliable Detection Against Ground Clutter," Tech. Publ. 156A, TRG Division of Control Data Corporation, Rosemont, Pa., Sept. 1964.
5. Applebaum, S.P., "Adaptive Arrays," Tech. Rept. SPL TR 66-1, Syracuse University Research Corporation, Syracuse, NY, 13210, Aug. 1966.
6. Nathanson, F.E., "Radar Design Principles," New York:McGraw-Hill, 1969.
7. Andrews, G.A., "Airborne Radar Motion Compensation Techniques, Evaluation of TACCAR," NRL Rept. 7407, Apr. 1972.
8. Blackman, R.B., and Tukey, J.W., "The Measurement of Power Spectra," New York: Dover Publ. 1958.



## DOCUMENT CONTROL DATA - R &amp; D

(Security classification of title, body of abstract and indexing annotation must be entered when the overall report is classified)

|   |  |  |                      |
|---|--|--|----------------------|
| 1. ORIGINATING ACTIVITY (Corporate author)<br>Naval Research Laboratory<br>Washington, D. C. 20375  |  | 2a. REPORT SECURITY CLASSIFICATION<br>Unclassified   |                      |
|   |  | 2b. GROUP  |                      |
| 3. REPORT TITLE<br>PERFORMANCE OF CASCADED MTI AND COHERENT INTEGRATION FILTERS IN A CLUTTER ENVIRONMENT  |  |  |                      |
| 4. DESCRIPTIVE NOTES (Type of report and inclusive dates)<br>This is an interim report on a continuing problem.   |  |  |                      |
| 5. AUTHOR(S) (First name, middle initial, last name)<br>G. A. Andrews, Jr.  |  |  |                      |
| 6. REPORT DATE<br>March 27, 1973  |  | 7a. TOTAL NO. OF PAGES<br>36   | 7b. NO. OF REFS<br>8 |
| 6a. CONTRACT OR GRANT NO.<br>R02-29   |  | 9a. ORIGINATOR'S REPORT NUMBER(S)<br>NRL Report 7533   |                      |
| b. PROJECT NO.<br>A360-5333/652B/2F00-141-601   |  |  |                      |
| c.  |  | 9b. OTHER REPORT NO(S) (Any other numbers that may be assigned this report)                                  |                      |
| d.  |  |  |                      |
| 10. DISTRIBUTION STATEMENT<br>Distribution limited to U.S. Government agencies only; test and evaluation; March 1973. Other requests for this document must be referred to the Director, Naval Research Laboratory, Washington, D.C. 20375  |  |  |                      |
| 11. SUPPLEMENTARY NOTES   |  | 12. SPONSORING MILITARY ACTIVITY<br>Department of the Navy Naval Air Systems Command, Washington, D.C. 20361 |                      |
| 13. ABSTRACT<br><p>The combination of moving target indicator (MTI) and coherent integration filters can provide velocity filtering with advantages that neither technique can provide alone. These techniques are evaluated as a special case of a transversal filter which lends itself to analysis using matrix algebra. This approach gives a simple, easily understood insight into the effects of weighting the input radar data. The resulting matrix equations are evaluated and the results are plotted for some special configurations. The computer programs which were written as a part of this research are not restricted to these configurations nor to the type of clutter spectrum that is assumed.</p> <p>It is shown that the performance of coherent integrators in a coherent noise (clutter) environment cannot be predicted with a concise analytical expression. In particular, the weighing of the input data and the covariance matrix of the interference determine the integrator performance.</p> |  |  |                      |

| 14. KEY WORDS  | LINK A |    | LINK B |    | LINK C |    |
|--|--------|----|--------|----|--------|----|
|  | ROLE   | WT | ROLE   | WT | ROLE   | WT |
| Radar<br>Doppler<br>Processing<br>Moving-Target Indicator (MTI)<br>Coherent integration<br>Filtering<br>Clutter<br>Rejection |        |    |        |    |        |    |





DEPARTMENT OF THE NAVY

NAVAL RESEARCH LABORATORY  
Washington, D.C. 20375

OFFICIAL BUSINESS

PENALTY FOR PRIVATE USE, \$300

POSTAGE AND FEES PAID  
DEPARTMENT OF THE NAVY  
DoD-316



DEPARTMENT OF THE NAVY  
NAVAL RESEARCH LABORATORY  
WASHINGTON, D.C. 20390

OFFICIAL BUSINESS  
NDW-NRL-5216/1534 (REV. 2-72)  
PENALTY FOR PRIVATE USE, \$300

POSTAGE AND FEES PAID  
DEPARTMENT OF THE NAVY



DoD-316

SUPERINTENDENT

U. S. NAVAL POSTGRADUATE SCHOOL

ATTN: TECHNICAL LIBRARY

MONTEREY, CALIFORNIA 93940 93943-5002

U152584